Characterization of the synchrotron-based 0.3-NA EUV microexposure tool at the ALS

Patrick Naulleau[1], Kenneth A. Goldberg[2], Erik Anderson[2], Kim Dean[3], Paul Denham[2], Jason P. Cain[4], Brian Hoef [2], Keith Jackson[2]

[1]College of Nanoscale Science and Engineering, University at Albany, NY 12220
[2]Center for X-Ray Optics, Lawrence Berkeley National Laboratory, Berkeley, CA 94720
[3]SEMATECH, Austin, TX 78741
[4]EECS Department, University of California, Berkeley, CA 94720

Abstract

Synchrotron-based EUV exposure tools continue to play a crucial roll in the development of EUV lithography. Utilizing a programmable-pupil-fill illuminator, the 0.3-NA microexposure tool at Lawrence Berkeley National Laboratory's Advanced Light Source synchrotron radiation facility provides the highest resolution EUV projection printing capabilities available today. This makes it ideal for the characterization of advanced resist and mask processes. The Berkeley tool also serves as a good benchmarking platform for commercial implementations of 0.3-NA EUV microsteppers because its illuminator can be programmed to emulate the coherence conditions of the commercial tools. Here we present the latest resist and tool characterization results from the Berkeley EUV exposure station.

1. Introduction

For volume nanoelectronics production using Extreme ultraviolet (EUV) lithography [1] to become a reality around the year 2011, advanced research tools are required today. Initial production tools are expected to have numerical apertures (NA) of 0.25 and be used for the 32-nm node. Relevant developmental systems thus also require NAs of 0.25 or higher. To meet the need for early development tools, microfield exposure systems trading off field size and speed for greatly reduced complexity have been developed. Similar microfield tools have been crucial

Contact: Patrick Naulleau
University at Albany, College of Nanoscale Science and Engineering,
255 Fuller Rd., Nanofab South, Albany, NY 12203
Tel: 518-437-8686 | Fax: 518-437-8603 | Email: Pnaulleau@uamail.albany.edu

to sub-0.2-NA EUV development in the past [2-4] and they currently serve as the only source for high-NA EUV printing [5-8].

System design for developemental tools can be further simplified by relying on synchrotron radiation as the EUV source instead of developmental stand-alone EUV sources. Although this approach does not provide any relevant EUV source learning, it does faclitate concentration on imaging and resist issues. The poor match between the intrinsic coherence properties of synchrotron radiation [9,10] and that required for lithographic imaging can readlily be dealt with using an active illuminator scheme [11].

In this paper we describe the latest results from the 0.3-NA EUV microfield exposure station at Lawrence Berkeley National Laboratory's Advanced Light Source synchrotron radiation facility. This static microfield exposure station utilizes SEMATECH's 5×-reduction, 0.3-NA Micro-Exposure Tool (MET) optic [12,13]. The MET optic has a well-corrected field of view of 1×3 mm at the reticle plane (200×600 mm at the wafer plane). At an operational resolution limit of approximately 30 to 35 nm, the latest printing results indicate that EUV performance is currently resist limited.

2. System overview

Figure 1 shows a CAD model depicting the major components of the exposure station along with the EUV beam path. The MET optic is a centrally-obscured (30% of the pupil radius) two-bounce system. The mask and wafer planes are tilted enabling the use of reflective masks. Using effectively coherent undulator radiation as the source, the system relies on a scanning illuminator [6, 14] to provide lithographically relevant coherence (pupil fill). The illuminator can generate arbitrary pupil fills covering a range up to 1.2 σ in x and 0.8 σ in y. Also, the central obscuration

alone can be illuminated, enabling frequency doubling from the mask to the wafer. For a detailed description of the exposure tool see Refs. 5 and 6.

3. Tool characterization

Because the above-described tool is, among other roles, intended for use in the development of EUV resist and mask processes, it is important to characterize the system performance and stability. For this task we choose to use one of the best performing EUV resists tested to date: Rohm and Hass *MET-1K* resist (XP3454C). This resist has been extensively characterized and reported on [6,15,16] over the past year and has been shown to have significantly better resolution then the previous generation of EUV resists such as Rohm and Haas *EUV-2D*.

Fine and stable focus control is crucial to obtaining useful data from the exposure tool. Figure 2 demonstrates the Berkeley tool capabilities in this area by showing a series of 40-nm lines and space images through focus in 30-nm steps. The illumination used for these prints was annular $0.3 < \sigma < 0.7$. The stable focus control is evident in the images themselves as well as in the extracted line-edge roughness (LER) and CD data [17].

Die-to-die performance serves as another mechanism for evaluating tool stability. Figure 3 shows CD and LER results from 100 identically exposed die (same dose and focus) on a single wafer. Figure 3(a) shows the measured CD for features coded as 60-nm across all 100 die. The error bars correspond to the variation observed from repeated measurements of the same die as well as line-to-line variations within a single image. The measured die-to-die rms CD variation is 1.2 nm. Assuming this CD variation to result from dose instability, this corresponds to a rms die-to-die dose variation of 1.5%, based on the previously measured CD sensitivity to dose. Figure 3(b) shows the LER from these same prints where we see the die-to-die variation to be

significantly smaller than the observed line-to-line variation depicted by the error bars. The results again indicate stable tool performance.

Flare remains a significant concern for EUV systems. Because the flare was not directly measured in the assembled MET optic, it is important to lithographically verify the predicted values. Although *MET-1K* is well suited for high-resolution work, its relatively low cross-linking threshold makes it unsuitable for characterization of flare. Not requiring high-resolution printing, flare tests can be implemented using Rohm and Haas *EUV-2D* resist. Figure 4 shows a direct comparison of the predicted and measured flare as a function of feature size. We find excellent agreement validating the predicted value of 7% flare in a 500-nm line within a 200×600-μm field. A more detailed description of the flare measurement can be found in the literature [18].

4. Resist-limited resolution

In the tool characterization section above there is no discussion of resolution limit. This is due to the fact that the achieved resolution is presently resist limited as opposed to tool limited. In this section we present data supporting this conclusion and present data from the highest resolving EUV resist tested in our system. Figure 5 shows the *Prolith* [19] calculated aerial-image image-log slope (ILS) and contrast as a function of feature size for equal lines and spaces. The *Prolith* model incorporates the latest wavefront data combining interferometric measurements obtained during alignment of the optic [20] and lithographic measurements of the latest state of the low order astigmatism and spherical error [21,22]. The illumination is assumed to be annular $0.3 < \sigma < 0.7$. For both the ILS and contrast we actually see the values to improve as the feature size shrinks from 35 to 25 nm. Figure 6 shows a series of equal line space images ranging from 45 to 25 nm printed in experimental *KRS* resist provided by IBM [23]. Although not as well characterized at EUV as *MET-1K*, EUV exposure tests consistently show *KRS* resist to slightly

outperform *MET-1K*, making it the highest resolving resist tested in our system. Contrary to the results in Fig. 5, it is evident that the imaging performance degrades rapidly for sizes below 35 nm, indicating a resist limit as opposed to an aerial-image limit.

Another way to assess a resist limited performance state is to probe printing performance as a function of aerial-image quality. Having a programmable pupil-fill illuminator, the Berkeley system is capable of producing large changes in aerial image quality at fixed feature sizes (Fig. 7). Comparing 35-nm imaging performance, we see that implementing monopole illumination to drive the aerial-image contrast up from approximately 50% to nearly 70% (y-monopole illumination), we can observe improved imaging performance. Performing the same comparison on 30-nm features, we see virtually no improvement in printing performance (pictures not shown) when going from 50% contrast to nearly 80% contrast (45°-monopole).

Given the resist limitations, it is evident that the optimal illumination choice for resolution enhancement on vertical features among the illumination types studied in Fig. 7 is y monopole because it provides the most contrast gain in the regime where the resist can still respond. Figure 8 shows a series of images recorded in *KRS* resist under y-monopole illumination, demonstrating resolving capabilities down to 32.5 nm for equal lines and spaces and 28 nm for semi-isolated lines.

5. Summary

Detailed characterization of the MET exposure tool at Berkeley indicates that the system is operating to specification. Printing results indicate that EUV performance is presently resist limited. The best resolving resist tested to date is capable of approximately 32.5-nm nested resolution and 28-nm isolated line resolution.

5. Acknowledgements

Special thanks are due to Robert Brainard and Thomas Koehler of Rohm and Haas as well as Greg Wallraff and Carl Larson of IBM for providing resist materials and expert processing support. We also acknowledge the entire CXRO staff for enabling this research. This research was performed at Lawrence Berkeley National Laboratory and supported by International Sematech. Lawrence Berkeley National Laboratory is operated under the auspices of the Director, Office of Science, Office of Basic Energy Science, of the US Department of Energy.

References

1. R. Stulen and D. Sweeney, IEEE J. Quantum Electron. **35**, 694-699 (1999).
2. J. Goldsmith, et al., Proc. SPIE **3676**, 264-271 (1999).
3. K. Hamamoto, T. Watanabe, H. Tsubakino, H. Kinoshita, T. Shoki, M. Hosoya, Journal of Photopolymer Science & Technology **14**, 567-572 (2001).
4. P. Naulleau, et al., J. Vac. Sci. & Technol. B **20**, 2829-2833 (2002).
5. P. Naulleau, et al., Proc. SPIE **5374**, 881-891 (2004).
6. P. Naulleau, et al., J. Vac. Sci. & Technol. B **22**, 2962-2965 (2004).
7. A. Brunton, et al., Proc. SPIE **5751**, *to be published* (2005).
8. H. Oizumi, Y. Tanaka, I. Nishiyama, H. Kondo, K. Murakami, Proc. SPIE **5751**, *to be published* (2005).
9. D. Attwood, et al., Appl. Opt. **32**, 7022-7031 (1993).
10. C. Chang, P. Naulleau, E. Anderson, and D. Attwood, Opt. Comm. **182**, 24-34 (2000).
11. P. Naulleau, K. Goldberg, P. Batson, J. Bokor, P. Denham, and S. Rekawa, Appl. Opt. **42**, 820-826 (2003).
12. J. Taylor, et al, 2nd International EUVL Workshop October 19-20, 2000 (http://www.sematech.org/resources/litho/meetings/euvl/20001019/707_SYS07_taylor.pdf)

13. R. Hudyma, J. Taylor, D. Sweeney, L. Hale, W. Sweatt, N. Wester, 2nd International EUVL Workshop October 19-20, 2000 (http://www.sematech.org/resources/litho/meetings/euvl/20001019/hudyma.pdf).
14. P. Naulleau, P. Denham, B. Hoef, and S. Rekawa, Opt. Comm. **234**, 53-62 (2004).
15. R. Brainard, T. Koehler, P. Naulleau, D. van Steenwinckel, Proc. SPIE **5751**, *to be published* (2005).
16. P. Naulleau, et al., Proc. SPIE **5751**, *to be published* (2005).
17. LER and CD analysis performed using the offline SEM analysis package SuMMIT, available from EUV Technology, Martinez, CA 94552, www.euvl.com/summit.
18. J. Cain, P. Naulleau, C. Spanos, Proc. SPIE **5751**, *to be published* (2005).
19. *Prolith* is a registered trademark of KLA-Tencor Corporation, San Jose, California 95134.
20. K. Goldberg, P. Naulleau, P. Denham, S. Rekawa, K. Jackson, E. Anderson, J. Liddle, J. Vac. Sci. & Technol. B **22**, 2956-2961 (2004).
21. P. Naulleau, J Cain, *submitted to J. Vac. Sci. & Technol. B* (2005).
22. P. Naulleau, J Cain, *in preparation* (2005).
23. Resist provided by G. Wallraff and C. Larson, IBM Almaden Research Ctr., San Jose, CA.

List of Figures

Fig. 1. Model depicting the major exposure station components and the EUV beam path (the system is described in detail in Ref. 6).

Fig. 2. Through-focus (30-nm steps) series of 40-nm lines and spaces in *MET-1K* resist under annular illumination. Also shown is a plot of the measured line-edge roughness (LER) and feature size through focus. The smooth behavior of the through-focus data is an indication of the good focus control performance.

Fig. 3. Die-to-die reproducibility of CD (a) and LER (b) on 60-nm coded lines and spaces printed in *MET-1K* resist.

Fig. 4. Direct comparison of measured and predicted flare in the MET optic. Lithographic measurement performed using the Kirk method.

Fig. 5. *Prolith* calculated aerial-image inage-log slope (ILS) and contrast as a function of feature size for equal lines and spaces. The model incorporates the latest wavefront data combining interferometric measurements obtained during alignment of the optic and lithographic measurements of the latest state of the low order astigmatism and spherical error. The illumination is annular 0.3-0.7.

Fig. 6. Equal line space images ranging from 45 to 25 nm printed in experimental *KRS* resist provided by IBM. Contrary to the results in Fig. 5, it is evident that the imaging performance degrades rapidly for sizes below 35 nm, indicating a resist limit as opposed to an aerial-image limit.

Fig. 7. Computed aerial-image contrast as a function of CD for three different pupil fills. Comparing 35-nm imaging performance, we see that implementing monopole illumination to drive the aerial-image contrast up from approximately 50% to nearly 70% (y-monopole illumination), we can observe improved imaging performance. Performing the same comparison on 30-nm features, we see virtually no improvement in printing performance (pictures not shown) when going from 50% contrast to nearly 80% contrast (45°-monopole).

Fig. 8. Images recorded in *KRS* resist under y-monopole illumination. (a) 35-nm lines and spaces, (b) 32.5-nm lines and spaces, (c) coded 27.5-nm lines 110-nm pitch, actual printed size in resist is 28.3-nm.

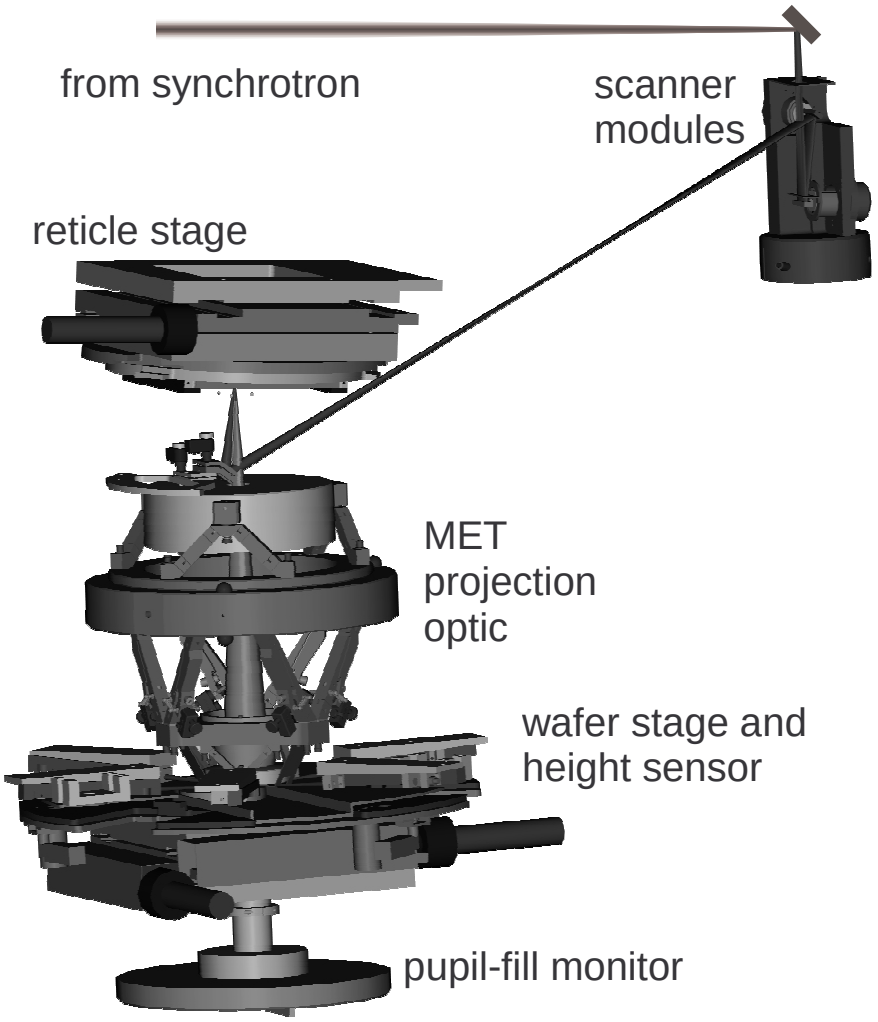

Fig. 1. Model depicting the major exposure station components and the EUV beam path (the system is described in detail in Ref. 6).

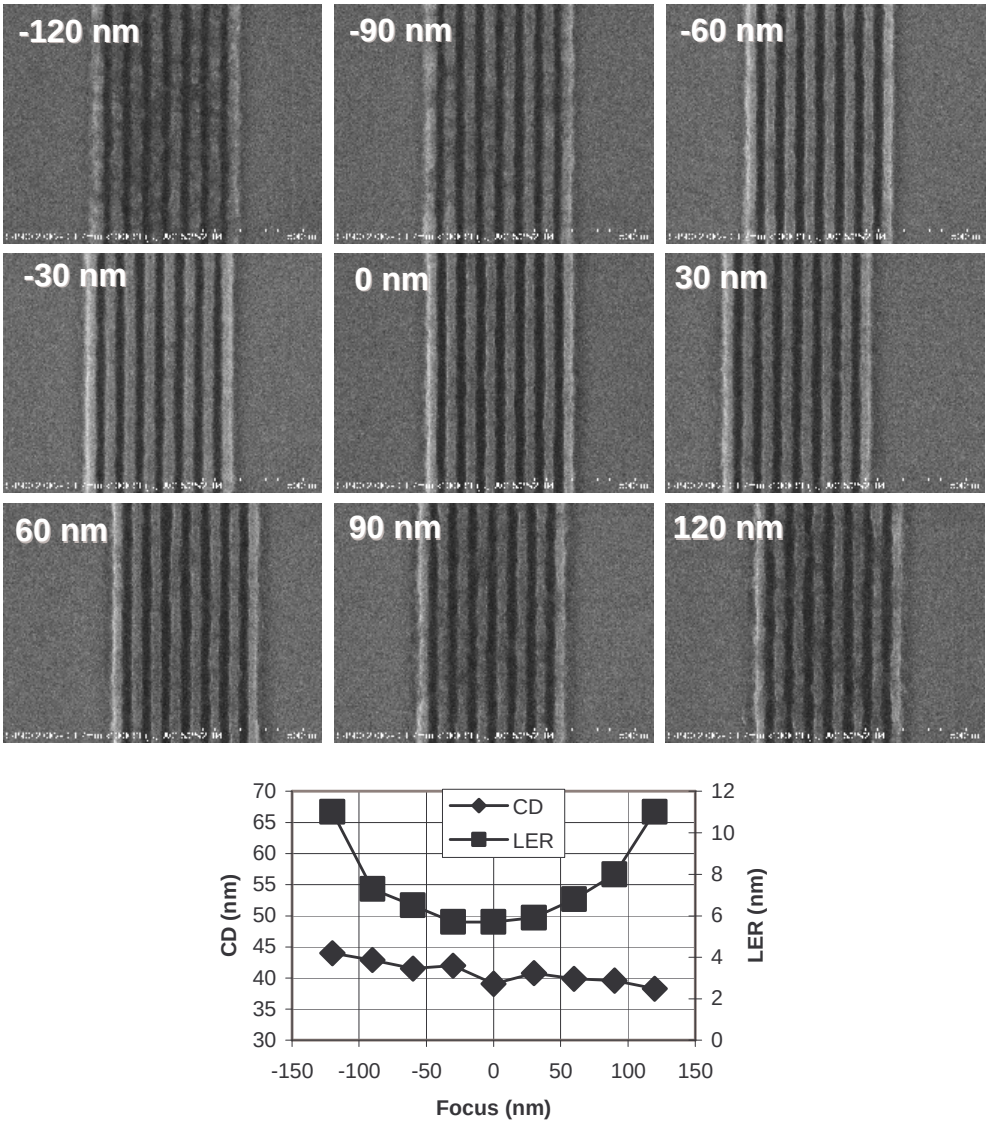

Fig. 2. Through-focus (30-nm steps) series of 40-nm lines and spaces in *MET-1K* resist under annular illumination. Also shown is a plot of the measured line-edge roughness (LER) and feature size through focus. The smooth behavior of the through-focus data is an indication of the good focus control performance.

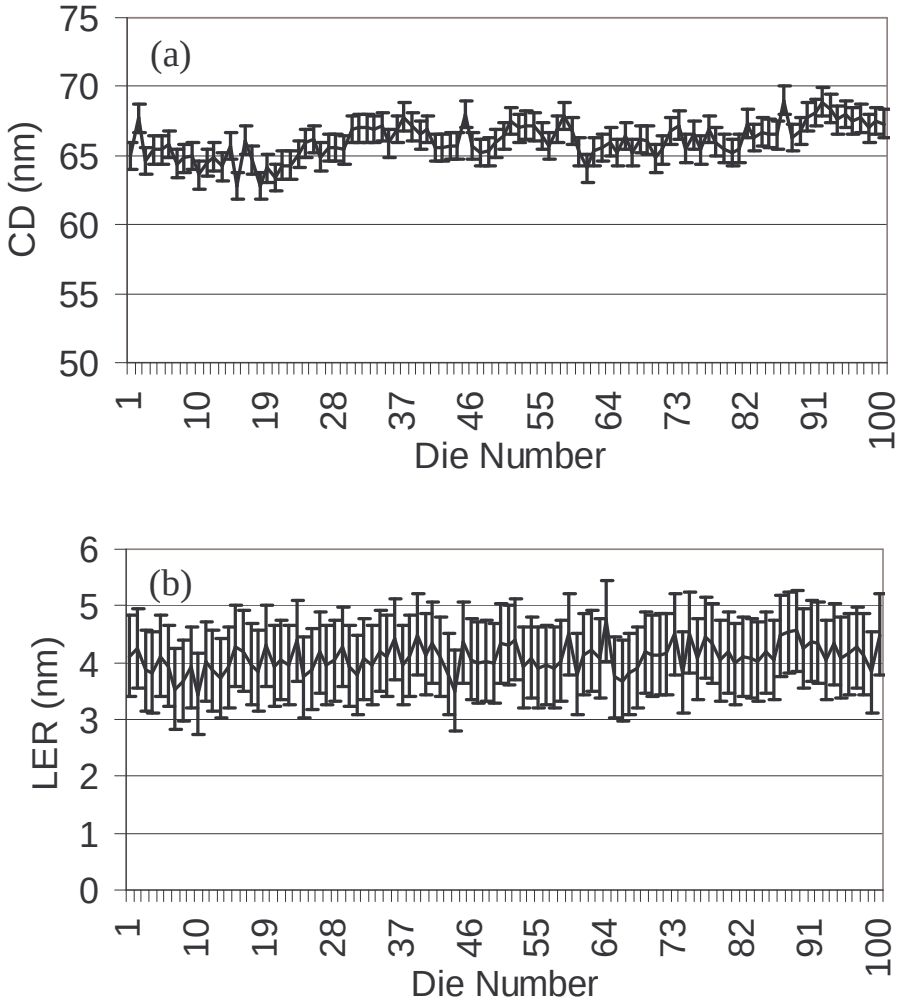

Fig. 3. Die-to-die reproducibility of CD (a) and LER (b) on 60-nm coded lines and spaces printed in *MET-1K* resist.

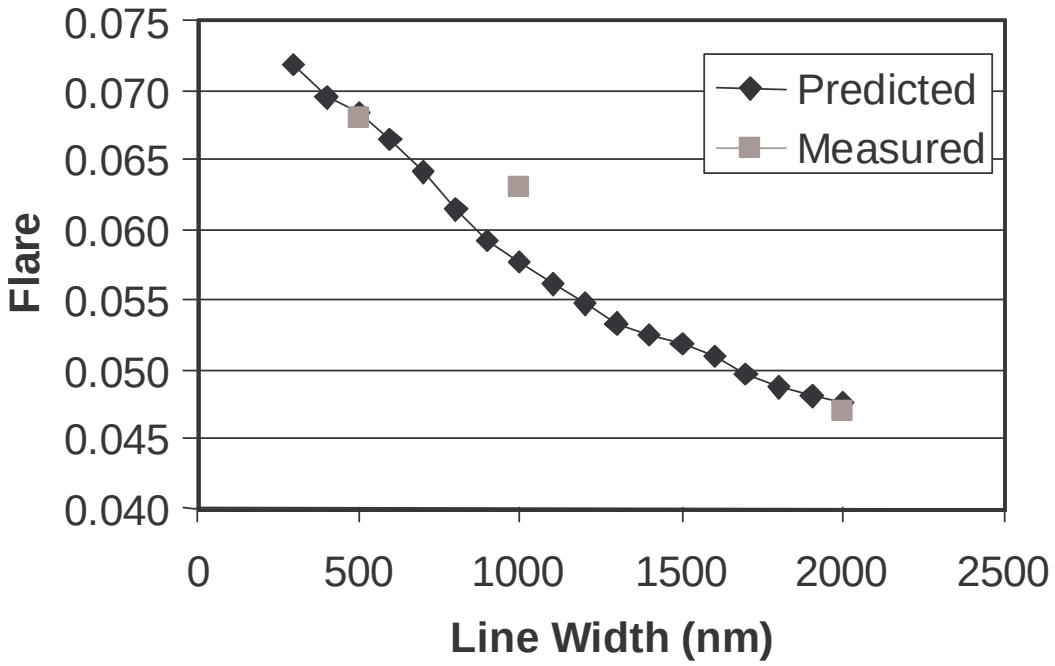

Fig. 4. Direct comparison of measured and predicted flare in the MET optic. Lithographic measurement performed using the Kirk method.

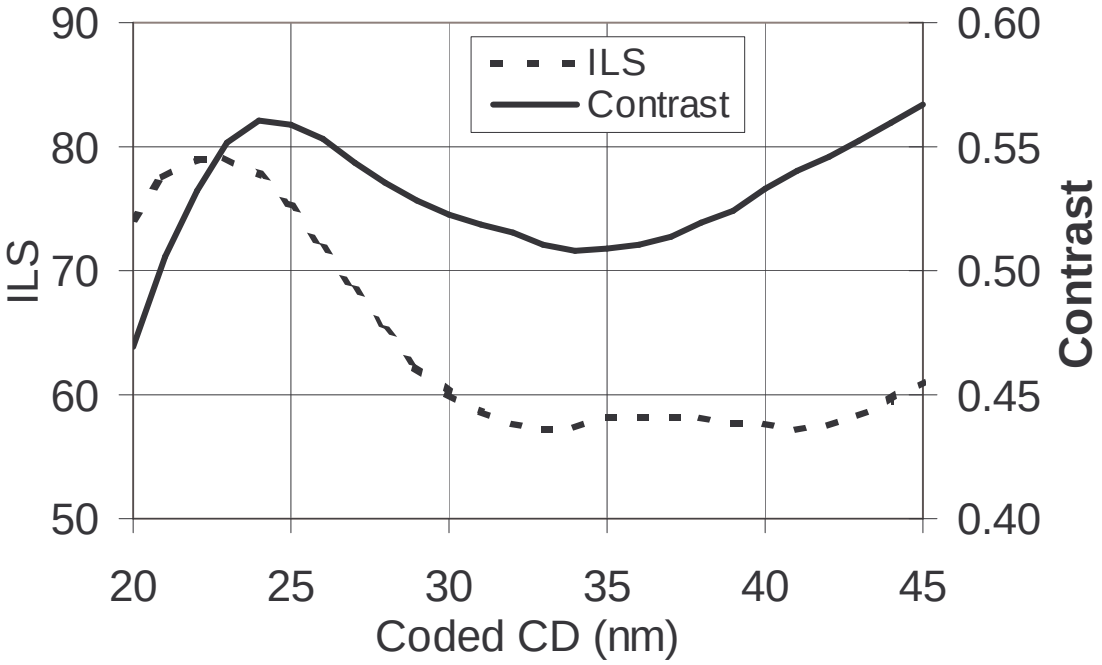

Fig. 5. *Prolith* calculated aerial-image inage-log slope (ILS) and contrast as a function of feature size for equal lines and spaces. The model incorporates the latest wavefront data combining interferometric measurements obtained during alignment of the optic and lithographic measurements of the latest state of the low order astigmatism and spherical error. The illumination is annular 0.3-0.7.

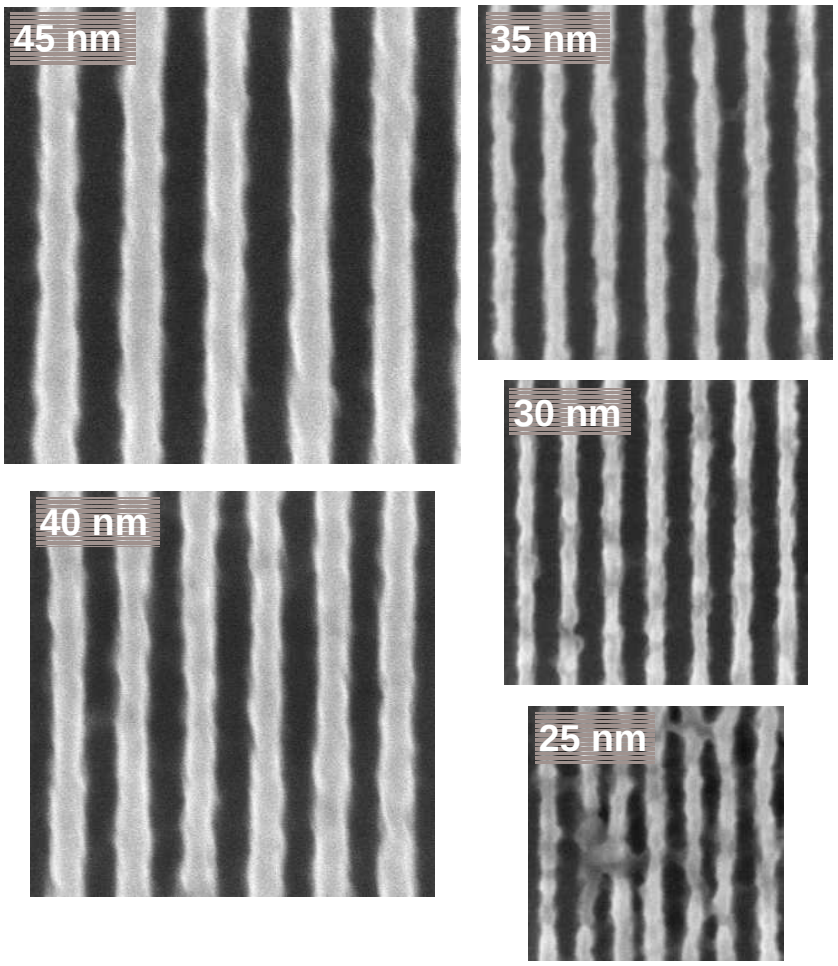

Fig. 6. Equal line space images ranging from 45 to 25 nm printed in experimental *KRS* resist provided by IBM. Contrary to the results in Fig. 5, it is evident that the imaging performance degrades rapidly for sizes below 35 nm, indicating a resist limit as opposed to an aerial-image limit.

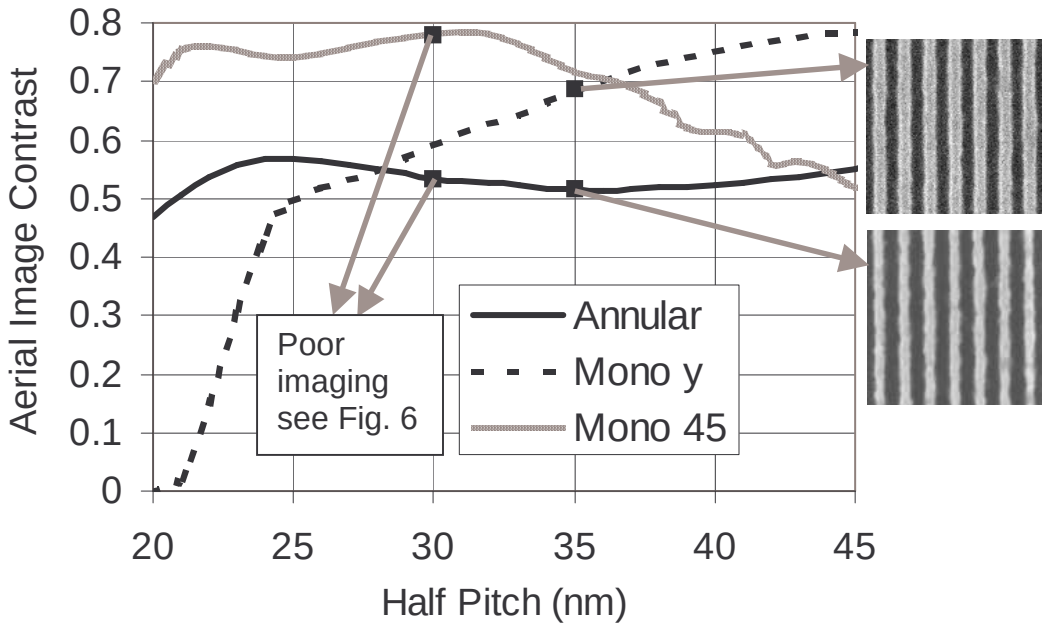

Fig. 7. Computed aerial-image contrast as a function of CD for three different pupil fills. Comparing 35-nm imaging performance, we see that implementing monopole illumination to drive the aerial-image contrast up from approximately 50% to nearly 70% (y-monopole illumination), we can observe improved imaging performance. Performing the same comparison on 30-nm features, we see virtually no improvement in printing performance (pictures not shown) when going from 50% contrast to nearly 80% contrast (45°-monopole).

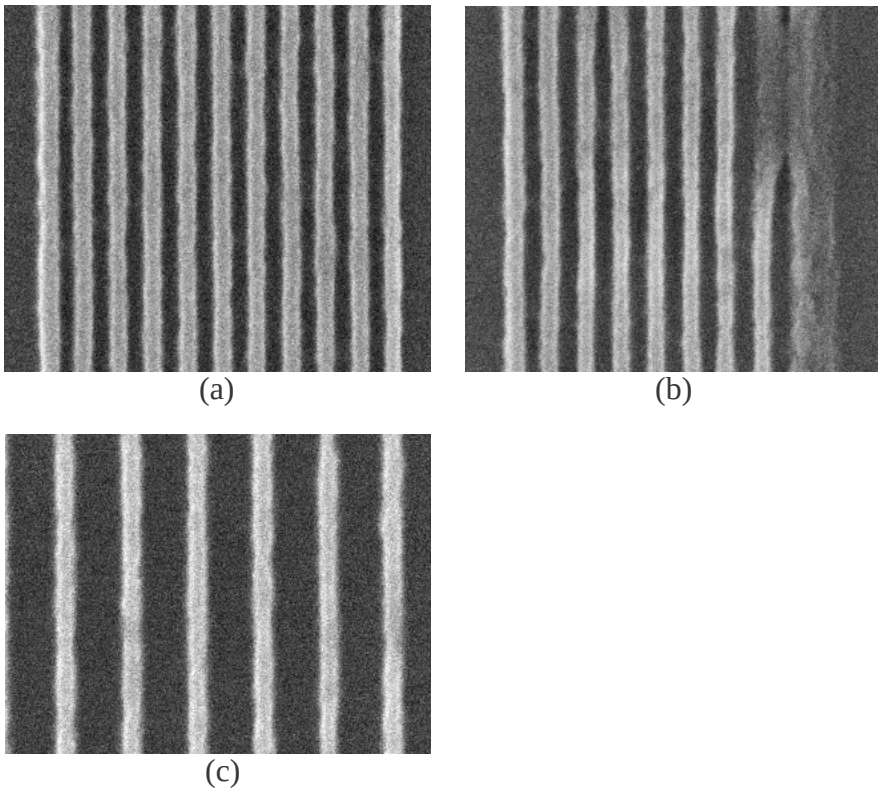

Fig. 8. Images recorded in *KRS* resist under y-monopole illumination. (a) 35-nm lines and spaces, (b) 32.5-nm lines and spaces, (c) coded 27.5-nm lines 110-nm pitch, actual printed size in resist is 28.3-nm.